International Journal of Internet, Broadcasting and Communication Vol.12 No.2 21-29 (2020)
http://dx.doi.org/10.7236/IJIBC.2020.12.2.21

IJIBC 20-2-4

Edge-Preserving and Adaptive Transmission Estimation for Effective Single Image Haze Removal

Jongho Kim

Professor, Department of Multimedia Engineering, Sunchon National University, Korea
jhkim@sunchon.ac.kr

Abstract

This paper presents an effective single image haze removal using edge-preserving and adaptive transmission estimation to enhance the visibility of outdoor images vulnerable to weather and environmental conditions with computational complexity reduction. The conventional methods involve the time-consuming refinement process. The proposed transmission estimation however does not require the refinement, since it preserves the edges effectively, which selects one between the pixel-based dark channel and the patch-based dark channel in the vicinity of edges. Moreover, we propose an adaptive transmission estimation to improve the visual quality particularly in bright areas like sky. Experimental results with various hazy images represent that the proposed method is superior to the conventional methods in both subjective visual quality and computational complexity. The proposed method can be adopted to compose a haze removal module for real-time devices such as mobile devices, digital cameras, autonomous vehicles, and so on as well as PCs that have enough processing resources.

Keywords: *Haze Removal, Edge-Preserving, Transmission Estimation, Visibility, Image Enhancement*

1. Introduction

Outdoor images are rapidly adopted in various fields such as smart transportation systems, (unmanned) aerial or drone image applications, video surveillance systems, and autonomous vehicles, etc. They are vulnerable to weather and environmental conditions such as fog, haze, smog, and so on. Additionally, the light reflected from the object is synthesized or scattered with the color of the suspended particles in the air, such that the contrast distortion or the color change of the image obtained through the camera is generated [1]. The improvement of the image visibility is strongly required for efficient implementation of a computer vision system using outdoor images. Simultaneously an appropriate level of computational complexity is needed to ensure the usefulness as the preprocessing [2]. Various haze removal methods have been studied to satisfy those conditions, and they can be classified into the plural image methods in the early stage and the single image methods actively studied recently.

As a plural image method, Schechner *et al*. proposed a haze removal method in [3] using the fact that haze

Manuscript Received: February. 17, 2020 / Revised: February. 21, 2020 / Accepted: February. 27, 2020
Corresponding Author: jhkim@sunchon.ac.kr
Tel: +82-61-750-3835, Fax: +82-61-750-3830
Professor, Department of Multimedia Engineering, Sunchon National University, Korea

values of two images acquired with different polarization filters at the same location are different. In spite of its good haze removal performance, it is limited for full-scale application due to the strong constraint that different polarization filters should be used at the same location even in a temporally changing hazy environment. Narasimhan *et al*. proposed a haze removal method in [4] based on the depth information obtained by using images taken under different weather conditions at the same location instead of polarization filters. Kopf *et al*. obtained depth information using the global positioning system (GPS) information embedded in the camera rather than an image, and proposed the haze removal method in [5] by calculating the haze concentration according to it.

In recent decades, the single image haze removal methods have been actively studied to consider the actual application of outdoor images [6-11]. They propose the approaches to restore the image from which the haze has been removed by satisfying additional assumptions and conditions [12-17]. The optical model widely used in the single image haze removal techniques are written as

$$\boldsymbol{I}(\boldsymbol{x}) = \boldsymbol{J}(\boldsymbol{x})t(\boldsymbol{x}) + \boldsymbol{A}(1 - t(\boldsymbol{x})) \tag{1}$$

where $\boldsymbol{x}$ is the pixel coordinates in vector form, $\boldsymbol{I}(\boldsymbol{x})$ is the observed hazy image acquired by a camera with three color channels, $\boldsymbol{J}(\boldsymbol{x})$ is the true radiance, i.e., the haze-free image to be restored, of the scene point imaged at $\boldsymbol{x}$, the atmospheric light $\boldsymbol{A}$ is a color value representing the ambient light in image area when $t(\boldsymbol{x}) = 0$, and the scene transmission $t(\boldsymbol{x})$, tightly related to the depth of each pixel, acts as a mixing coefficient between the scene radiance $\boldsymbol{J}(\boldsymbol{x})$ and the atmospheric light $\boldsymbol{A}$. The transmission modelled by $t(\boldsymbol{x}) = e^{-\beta d(\boldsymbol{x})}$ denotes the percentage of light received by the camera from $\boldsymbol{J}(\boldsymbol{x})$, and $d(\boldsymbol{x})$ is the distance from the scene point to the camera and β is the attenuation coefficient of the atmosphere. Generally, β is dependent on wavelength and therefore $t(\boldsymbol{x})$ is different per color channel [3]. This dependency has been assumed negligible in previous single image dehazing methods including this work to reduce the number of unknowns and we follow this assumption.

Single image haze removal can be regarded as a problem of estimating $\boldsymbol{A}$ and $t(\boldsymbol{x})$ from $\boldsymbol{I}(\boldsymbol{x})$, and using them to restore $\boldsymbol{J}(\boldsymbol{x})$. Based on the optical model of (1), Tan's method focuses on enhancing the visibility of the image in [7]. The transmission $t(\boldsymbol{x})$ in a local patch is estimated by maximizing the visibility under a constraint that the intensity of $\boldsymbol{J}(\boldsymbol{x})$ is less than the intensity of $\boldsymbol{A}$, and then the Markov Random Fields (MRF) model is used to further regularize the result. This approach is able to greatly unveil details and structures from hazy images. However, the output images usually tend to have large saturation values, and they may contain halo effects near the depth discontinuities. Fattal proposes an approach in [8] based on Independent Component Analysis (ICA). The albedo of a local patch is assumed to be a constant, and thus all vectors of $\boldsymbol{J}(\boldsymbol{x})$ in the patch have the same direction, which is estimated by ICA by assuming that the statistics of the surface shading $||\boldsymbol{J}(\boldsymbol{x})||$ and the transmission $t(\boldsymbol{x})$ are independent in the patch. The MRF model guided by the input color image is applied to extrapolate the solution to the whole image. This approach is physics-based and can produce a natural haze-free image together with a good depth information. However, any lack of variation or low signal-to-noise ratio (often in dense haze region) makes the statistics unreliable, since the statistical independent components vary significantly. Moreover, as the statistics is based on color information, it is invalid for grayscale images and it is difficult to handle dense haze that is colorless.

Through observation of haze-free images, He *et al*. proposed a dark channel prior (DCP) in [9] for image dehazing, that is, the dark channel of a haze-free image in each pixel is assumed to be zero. The transmission $t(\boldsymbol{x})$ can be estimated on the basis of the DCP. To reduce the halo effect caused by the local minimum operation, the soft matting optimization method refining the transmission. The soft matting is an iterative optimization process that requires a lot of computations, even though this method achieves a state-of-the-art haze removal performance. Moreover, for the bright sky regions, the DCP is not valid, and thus the contour artifacts can sometimes be observed because of the failure of the DCP in those regions.

To improve the DCP-based method, we develop a direct transmission estimation without a refinement process, which greatly reduces the processing time. When computing the dark channel in the edge area, it is obtained through the patch-level computation so that our method can avoid over-saturation while preserving edges. An adaptive transmission estimation is proposed to compensate for sky regions. In this paper, we propose a novel framework for single image haze removal, in which both the computation time and quality performance are improved compared to the conventional DCP-based method. The proposed method includes two novel contributions as explained below:

- To reduce the halo effect caused by the local patch operation, a novel method called edge-preserving transmission estimation is developed for dark channel computation. This results in a direct estimation of the fine transmission with an edge-preserving property. Compared to the computationally expensive refinement method in [9], our method drastically reduce the computing time for the fine transmission without any refinement process.
- An adaptive transmission estimation is proposed to compensate for the failure of the DCP in the sky regions. Modelled by a Gaussian function, it is the same as the conventional DCP for the pixels in non-sky regions while it can produce a more accurate prior for pixels in the sky and other bright regions.

The rest of the paper is organized as follows. In Section 2, related works of DCP are briefly reviewed, and then our proposed method is presented in detail. The experimental results and analysis are shown in Section 3. Finally, the concluding remarks are given in Section 4.

2. Proposed Haze Removal Method

2.1 DCP-Based Haze Removal Method

The DCP is derived from the observation that many pixels have a value close to zero in at least one of R, G, B channels of a haze-free image. He *et al.* defines the patch-based dark channel to reflect the observation as

$$J^{dark}(\boldsymbol{x}) = \min_{\boldsymbol{y}\in\Omega(\boldsymbol{x})}\left(\min_{c\in\{r,g,b\}} J^{c}(\boldsymbol{y})\right) \tag{2}$$

where $\Omega(\boldsymbol{x})$ is a local patch centered at $\boldsymbol{x}$, $\boldsymbol{y}$ denotes the index for a pixel in the patch, c is one of the three color channels (r, g, b), and $J^c(\boldsymbol{x})$ means the color channel c of $\boldsymbol{J}(\boldsymbol{x})$ [9]. $J^{dark}(\boldsymbol{x})$ in (2) can be reduced to zero according to the definition of DCP, and we utilize it as additional information for the single image haze removal. In order to use DCP, we apply the minimum operation to both sides of (1), then divide it by $\boldsymbol{A}$ to yield

$$\min_{\boldsymbol{y}\in\Omega(\boldsymbol{x})}\left(\min_{c}\frac{I^c(\boldsymbol{y})}{A^c}\right) = t(\boldsymbol{x})\min_{\boldsymbol{y}\in\Omega(\boldsymbol{x})}\left(\min_{c}\frac{J^c(\boldsymbol{y})}{A^c}\right) + 1 - t(\boldsymbol{x}). \tag{3}$$

Applying the DCP to (3), the first term on the right side is 0, so we can estimate the transmission as

$$t(\boldsymbol{x}) = 1 - \min_{\boldsymbol{y}\in\Omega(\boldsymbol{x})}\left(\min_{c}\frac{I^c(\boldsymbol{y})}{A^c}\right). \tag{4}$$

Since the transmission $t(\boldsymbol{x})$ is calculated in units of patches in (4), its edge information does not match to that of the original image. This makes the blocking effects, which consequently cause a halo effect in the restored image. A refinement process is included to overcome this problem, and He *et al.* refine the transmission, a coarse data at this time, based on the similarity in their form between the optical model of hazy images in (1) and the matting equation. He *et al*. introduce the matting technique proposed by Levin *et al*. However, when the total number of pixels is N, it includes a very large matrix of $N \times N$, resulting in a large memory requirement and computation complexity. Actually, Levin *et al*. apply the matting technique to the images with reduced resolutions in order to overcome the limitation of memory space for the large size images, such as larger than 400×400, and the interpolation is then used to reconstruct the image [18]. After the refinement process, $\boldsymbol{J}(\boldsymbol{x})$ can be restored by (1). We first pick the top 0.1% brightest pixels in the dark channel. Among these pixels, usually most haze-opaque, a pixel with the highest intensity in the input image $\boldsymbol{I}(\boldsymbol{x})$ is selected as the atmospheric light $\boldsymbol{A}$. Note that this pixel may not be brightest one in the whole input image.

2.2 Edge-Preserving Transmission Estimation

The patch-based dark channel includes distortions in the transmission estimation, since it does not reflect the edge information accurately, even though it is advantageous for the atmospheric light estimation. On the other hand, the pixel-based dark channel has a problem for the atmospheric light estimation, while it can estimate the transmission faithfully reflecting the edge information. Our work proposes an effective transmission estimation while preserving the edge information with combination of both methods. The patch-based dark channel of the input image, $I^d(\boldsymbol{x})$ can be obtained by using

$$I^d(\boldsymbol{x}) = \min_{\boldsymbol{y} \in \Omega(\boldsymbol{x})} \left(\min_{c \in \{r,g,b\}} I^c(\boldsymbol{y}) \right) \tag{5}$$

where c denotes one of the three color channels, and $I^c(\boldsymbol{x})$ denotes the color channel c of $\boldsymbol{I}(\boldsymbol{x})$. The pixel-based dark channel of the input image, $I^{pd}(\boldsymbol{x})$ is defined as

$$I^{pd}(\boldsymbol{x}) = \min_{c \in \{r,g,b\}} I^c(\boldsymbol{x}). \tag{6}$$

We can estimate the transmission preserving the edge information for the patch $\Omega(\boldsymbol{x})$, by comparing $I^d(\boldsymbol{x})$ of (5) and $I^{pd}(\boldsymbol{x})$ of (6) in a pixel-based fashion, and selecting a large value. In the homogeneous region belonging to the same object as the left patch in Figure 1(a), the difference between $I^d(\boldsymbol{x})$ and $I^{pd}(\boldsymbol{x})$ is small, so that it operates in the same manner as the existing patch-based method. As the right patch in Figure 1(a), we select either $I^d(\boldsymbol{x})$ or $I^{pd}(\boldsymbol{x})$ in a pixel-based fashion near the edge, and thus a dark channel preserving edge information can be obtained. The conventional patch-based method selects the minimum value in the patch along the edges of the objects as shown in Figure 1(b), which leads the loss of edge information. Our method compares $I^d(\boldsymbol{x})$ and $I^{pd}(\boldsymbol{x})$, and then selects a large value for each pixel in the patch, so that it can obtain the dark channel while preserving the edge information, as shown in Figure 1(c).

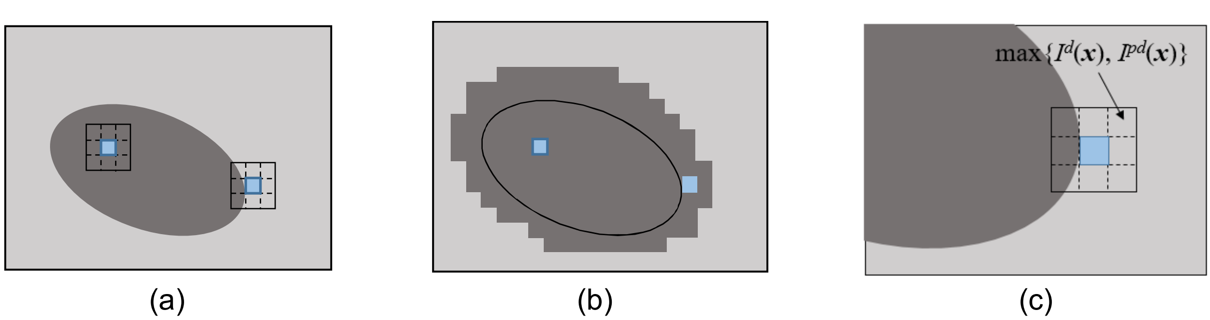

Figure 1. Comparative illustration of the dark channel method. (a) Distribution of the object and patches, (b) Patch-based dark channel method, (c) Proposed dark channel method

The proposed method estimates the transmission for the changing areas such as near the edges in a pixel-based manner, and thus does not require the refinement process to reduce the halo effect of the restored image. Consequently, it can greatly reduce the computational complexity compared to the conventional method.

2.3 Adaptive Transmission Estimation

The other drawback of the conventional DCP is that the contour artifacts may occur in a restored haze-free image, apart from the time-consuming refinement process. Since the $I^d(\boldsymbol{x})$ in the sky region is usually close to the atmospheric light $\boldsymbol{A}$, that is, $I^d(\boldsymbol{x})/\boldsymbol{A}$ is close to 1, it results in a very small transmission $t(\boldsymbol{x})$ according to (4). When restored by (1), this leads that $\boldsymbol{J}(\boldsymbol{x})$ can be greatly changed, even the small local intensity difference in sky region. This can be an idea for how the contour artifacts occur in a sky region. Due to the dark channel of the haze-free images in the bright or sky areas is far from 0, the DCP fails to correctly estimate the transmission $t(\boldsymbol{x})$ in those regions, which can be expressed as

$$t(\boldsymbol{x}) = \left(1 - \frac{I^d(\boldsymbol{x})}{\boldsymbol{A}}\right) / \left(1 - \frac{J^{dark}(\boldsymbol{x})}{\boldsymbol{A}}\right). \tag{7}$$

To deal with this case, a confidence value obtained through a sophisticated human vision-based assumption is introduced in [17] to recompute the dark channel of the haze image $I^d(\boldsymbol{x})$. It can reduce the contour artifacts by decreasing the $I^d(\boldsymbol{x})$ in the sky regions, but it also decreases the dark channel to some extent in non-sky regions, which may lead to the over-estimation of the transmission. Instead of modifying the $I^d(\boldsymbol{x})$, we solve this problem more essentially by making a new assumption for the dark channel $J^{dark}(\boldsymbol{x})$ in the haze-free images. We use a function of $I^d(\boldsymbol{x})$ to estimate $J^{dark}(\boldsymbol{x})$, since the only input is $I^d(\boldsymbol{x})$ of the hazy image. The estimated $J^{dark}(\boldsymbol{x})$ is then close to zero in a non-bright area and is of high value in a bright area, which can eliminate the contour artifacts in the sky regions as well as not violate the conventional DCP in non-sky regions. The idea is that for the pixels in the sky regions, $J^{dark}(\boldsymbol{x})$ is usually close to the atmospheric light $\boldsymbol{A}$. We use the Gaussian function of $(1 - I^d(\boldsymbol{x})/\boldsymbol{A})$ instead of setting $J^{dark}(\boldsymbol{x})/\boldsymbol{A}$ to 0, defined in (8), so that we can adaptively set $J^{dark}(\boldsymbol{x})/\boldsymbol{A}$ close to zero when the pixels are in non-sky regions and to a high value in the sky regions by using a small σ value.

$$\frac{J^{dark}(\boldsymbol{x})}{\boldsymbol{A}} = g\left(1 - I^d(\boldsymbol{x})/\boldsymbol{A}\right) = ke^{-\frac{\left(1 - I^d(\boldsymbol{x})/\boldsymbol{A}\right)^2}{\sigma^2}}, \tag{8}$$

and the transmission can be estimated using (7) and (8) as

$$t(\boldsymbol{x}) = \left(1 - \alpha\frac{I^d(\boldsymbol{x})}{\boldsymbol{A}}\right) \Bigg/ \left(1 - k\exp\left(-\frac{\left(1 - I^d(\boldsymbol{x})/\boldsymbol{A}\right)^2}{\sigma^2}\right)\right). \tag{9}$$

We empirically set σ to 0.15, and α is set to keep a bit of haze to make the restored image appear more natural. Since $J^{dark}(\boldsymbol{x})/\boldsymbol{A}$ is smaller than $I^d(\boldsymbol{x})/\boldsymbol{A}$, k is set to prevent $J^{dark}(\boldsymbol{x})/\boldsymbol{A}$ from being too large. For estimation of the atmospheric light $\boldsymbol{A}$, we use the same method as in [9] by using the highest intensity pixel from the input image among the top 0.1% of the brightest pixels in the dark channel. The final haze-free image $\boldsymbol{J}(\boldsymbol{x})$ can be recovered by using (1). The recommended values for α and k are 0.85 – 0.95 and 0.4 – 0.6, respectively.

3. Experimental Results

We evaluate the performance of the proposed haze removal algorithm with widely-used hazy images, and compare it with the existing methods. The performance evaluation is conducted in terms of subjective visual quality and computational complexity that is measured by PC-based execution time. The existing methods included in comparison are Tan's method, maximizing local contrast of hazy images in [7], Fattal's method, assuming the transmission and the surface shading locally uncorrelated in [8], and He *et al.*'s method, using the patch-based DCP in [9]. However, He *et al.*'s method includes the downsampling and interpolation processing for refinement of the images larger than 400×400 pixels due to memory amount restriction, and we consider them as a part of the whole execution time. Moreover, the patch size of the proposed method is set to 7×7 pixels smaller than that of the conventional method.

It is shown in Figures 2 and 3 that the results of the haze removal methods including the proposed method applied to the test hazy images for the subjective visual quality evaluation. Figure 2 represents the small depth difference between the objects and background, whereas the depth difference in Figure 3 is relatively large, which also contains the sky area. Tan's method increases the contrast in the result image, however color saturation occurs in the scene far from camera as shown in Figures 2(b) and 3(b). Compared to the input image, Fattal's method increases the brightness due to consideration of image reflection rate, however the result image looks partially blurry, particularly in areas far from camera as shown in Figures 2(c) and 3(c). This is noticeable in images with large depth difference, such as Figure 3(c). He *et al.*'s method is excellent in haze removal performance, however the restored image remains somewhat hazy as shown in Figure 2(d), or it looks relatively dark in areas far from camera as shown in Figure 3(d). It can be seen in Figures 2(e) and 3(e) that the proposed method improves visibility and recognizes the objects better without saturation of particular color channel by effective haze removal.

(a) (b) (c) (d) (e)

Figure 1. Visual quality comparison of haze removal results for *Red Bricks House* (a) Hazy input image (b) Tan's method (c) Fattal's method (d) He *et al.*'s method (e) Proposed method

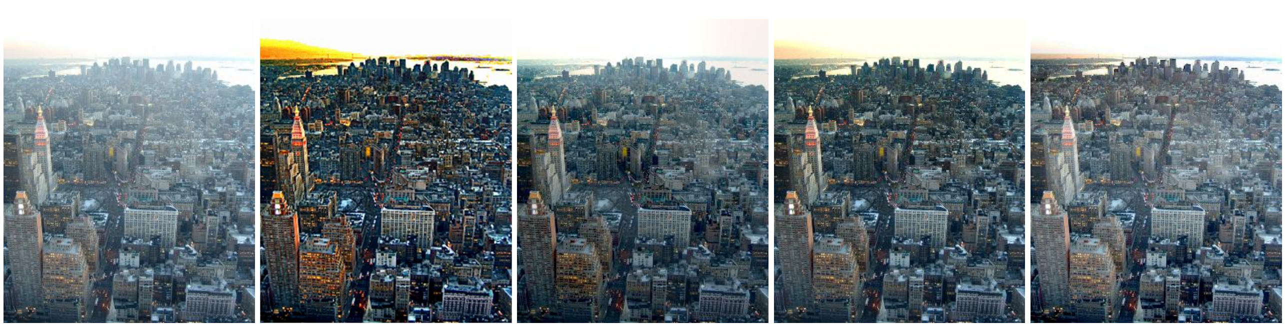

(a) (b) (c) (d) (e)

Figure 2. Visual quality comparison of haze removal results for *Manhattan* (a) Hazy input image (b) Tan's method (c) Fattal's method (d) He *et al.*'s method (e) Proposed method

The analysis results of computational complexity for the conventional methods and the proposed algorithm are listed in Table 1. The computational complexity is measured by execution time of software implementation for each method. The simulation is carried out on the PC of 2.8GHz CPU and 3.5GB memory with 32-bit operating system and the software is implemented with C++ language. We execute the software 10 times for each image and obtain the average execution time.

Table 1. Comparative analysis for execution time (in sec) of each haze removal method

Image	Tan	Fattal	He *et al.*	Proposed
cityscape	59.81	10.97	9.85	2.51
forest	152.11	22.31	15.32	6.11
landscape	70.15	14.04	11.79	4.63
manhattan1	113.26	18.36	12.62	4.87
manhattan2	144.87	20.72	14.21	5.65
mountain	63.63	12.12	9.96	3.08
pumpkins	76.08	13.93	10.28	3.72
red bricks house	72.31	13.88	10.21	3.56
tiananmen	66.24	12.63	9.72	2.88
train	62.63	11.92	9.28	2.43
wheat cones	67.38	12.71	9.57	2.79
yosemite1	98.35	15.35	10.41	5.24
average	87.24	14.92	11.10	3.96

It can be found from Table 1 that the execution time of the proposed algorithm are greatly reduced compared to the conventional methods, particularly He *et al.*'s method. It is caused by two factors: the small patch size (7×7) reduces the computational complexity of the method; the edge-preserving transmission estimation does not require the refinement process which takes the execution time greatly. There are two points of views: the visual quality of the restored images and the computational complexity of the algorithm. It can be seen in Figures 2 and 3 that the proposed haze removal method makes visual quality of the restored images better compared to the conventional methods, and thus it improves the visibility of objects. Also, it can be thought from Table 1 that the execution time of the proposed haze removal method is greatly improved compared to the existing methods, and thus is can be applied to various devices utilizing outdoor images, such as autonomous vehicles, drones and unmanned aerial vehicles imaging, video surveillance systems, etc.

4. Conclusions

This paper presents an effective single image haze removal algorithm using edge-preserving and adaptive transmission estimation, so that it enhances the visibility of outdoor images vulnerable to weather and environmental conditions such as fog, smog, haze, etc., and it can be implemented with low computational complexity. The low complexity implementation of the proposed method can be achieved by using the small patch size and by not use of the refinement process. The edge-preserving transmission estimation does not the refinement process that requires large amount of memory and computational complexity, and it can consequently restore the hazy images without halo effects. Moreover, we propose an adaptive transmission estimation to enhance the visual quality particularly in bright regions like sky.

Comprehensive experiments with various hazy images show in the results that the proposed method is superior to both perspectives: subjective visual quality and computational complexity. The proposed haze removal method compared to the conventional methods shows the better visual quality and the low computational complexity measured by PC-based execution time. The proposed method can be adopted to compose a haze removal module for real-time working in mobile devices, digital cameras, and so on as well as PCs that have enough processing resources. Further research topics related to this paper will be studied with color lines and haze lines methods to improve the visual quality of restored images, and with the low complexity implementation methods as well.

Acknowledgement

This work was supported by Basic Science Research Program through the National Research Foundation of Korea (NRF) funded by the Ministry of Education (NRF-2018R1D1A3B07050086).

References

[1] C. Yeh, L. Kang, M. Lee, and C. Lin, "Haze effect removal from image via haze density estimation in optical model," *Optics Express*, Vol. 21, No. 22, pp. 27127-27141, Nov. 2013.
DOI: http://dx.doi.org/10.1364/OE.21.027127

[2] J. Tarel and N. Hautiere, "Fast visibility restoration from a single color or gray level images," in *Proc. IEEE Int. Conference on Computer Vision (ICCV)*, pp. 2201-2208, Sep. 29-Oct. 2, 2009.
DOI: http://dx.doi.org/10.1109/ICCV.2009.5459251

[3] Y. Schechner, S. Narasimhan, and S. Nayer, "Instant dehazing of images using polarization," in *Proc. IEEE Conference on Computer Vision and Pattern Recognition (CVPR)*, pp. 325-332, Dec. 8-14, 2001.
DOI: http://dx.doi.org/10.1109/CVPR.2001.990493

[4] S. Narasimhan and S. Nayer, "Contrast restoration of weather degraded images," *IEEE Trans. Pattern Analysis and Machine Intelligence*, Vol. 25, No. 6, pp. 713-724, June 2003.
DOI: http://dx.doi.org/10.1109/TPAMI.2003.1201821

[5] J. Kopf, B. Neubert, B. Chen, M. Cohen, D. Cohen-Or, O. Deussen, M. Uyttendaele, and D. Lischinski, "Deep photo: Model-based photograph enhancement and viewing," *ACM Trans. Graphics*, Vol. 27, No. 5, pp. 116:1-116:10, Dec. 2008.
DOI: http://dx.doi.org/10.1145/1409060.1409069

[6] S. Lee, S. Yun, J. Nam, C. Won, and S. Jung, "A review on dark channel prior based image dehazing algorithms," *The European Association for Signal Processing (EURASIP) Journal on Image and Video Processing*, Vol. 2016, No. 4, pp. 1-23, Dec. 2016.
DOI: http://dx.doi.org/10.1186/s13640-016-0104-y

[7] R. Tan, "Visibility in bad weather from a single image," in *Proc. IEEE Conference on Computer Vision and Pattern Recognition (CVPR)*, pp. 1-8, June 23-28, 2008.
DOI: http://dx.doi.org/10.1109/CVPR.2008.4587643

[8] R. Fattal, "Single image dehazing," *ACM Trans. Graphics*, Vol. 27, No. 3, pp. 1-9, Aug. 2008.
DOI: http://dx.doi.org/10.1145/1360612.1360671

[9] K. He, J. Sun, and X. Tand, "Single image haze removal using dark channel prior," *IEEE Trans. Pattern Analysis and Machine Intelligence*, Vol. 33, No. 12, pp. 2341-2353, Dec. 2011.
DOI: http://dx.doi.org/10.1109/TPAMI.2010.168

[10] J. Kim, "Histogram modification based on additive term and gamma correction for image contrast enhancement," *Journal of the Korea Institute of Electronic Communication Science*, Vol. 13, No. 5, pp. 1117-1124, Oct. 2018.

[11] J. Kim, "Single image haze removal algorithm using dual DCP and adaptive brightness correction," *Journal of the Korea Academia-Industrial cooperation Society (JKAIS)*, Vol. 19, No. 11, pp. 31-37, Nov. 2018.
DOI: http://dx.doi.org/10.5762/KAIS.2018.19.11.31

[12] W. Oh and J. Kim, "Single image haze removal technique via pixel-based joint BDCP and hierarchical bilateral filter," *Journal of the Korea Institute of Electronic Communication Science*, Vol. 14, No. 1, pp. 257-264, Feb. 2019.

[13] J. Kim, "Efficient single image dehazing by pixel-based JBDCP and low complexity transmission estimation," *Journal of the Korea Institute of Electronic Communication Science*, Vol. 14, No. 5, pp. 977-984, Oct. 2019.

[14] J. Kim, "Low complexity single image dehazing via edge-preserving transmission estimation and pixel-based JBDC," *Journal of the Korea Academia-Industrial cooperation Society (JKAIS)*, Vol. 20, No. 12, pp. 1-7, Dec. 2019.
DOI: http://dx.doi.org/10.5762/KAIS.2019.20.12.1

[15] T. Yu, I. Riaz, J. Piao, and H. Shin, "Real-time single image dehazing using block-to-pixel interpolation and adaptive dark channel prior," *IET Image Processing*, Vol. 9, No. 9, pp. 725-734, Sep. 2015.
DOI: http://dx.doi.org/10.1049/iet-ipr.2015.0087

[16] S. Salazar-Colores, J. Ramos-Arreguin, J. Pedraza-Ortega, and J. Rodriguez-Resendiz, "Efficient single image dehazing by modifying the dark channel prior," *The European Association for Signal Processing (EURASIP) Journal on Image and Video Processing*, Vol. 2019:66, No. 1, pp. 1-8, May 2019.
DOI: http://dx.doi.org/10.1186/s13640-019-0447-2

[17] B. Li, S. Wang, J. Zheng, and L. Zheng, "Single image haze removal using content-adaptive dark channel and post enhancement," *IET Computer Vision*, Vol. 8, No. 2, pp. 131-140, Apr. 2014.
DOI: http://dx.doi.org/10.1049/iet-cvi.2013.0011

[18] A. Levin, D. Lischinski, and Y. Weiss, "A closed form solution to natural image matting," *IEEE Trans. Pattern Analysis and Machine Intelligence*, Vol. 30, No. 2, pp. 228-242, Feb. 2008.
DOI: http://dx.doi.org/10.1109/TPAMI.2007.1177